# Electronic Supplementary Information

# Sulfur doped $Co/SiO_2$ catalysts for chirally selective synthesis of single walled carbon nanotubes

**Hong Wang,[a] Kunli Goh,[a] Dingshan Yu,[a] Wenchao Jiang,[a] Raymond Lau,[a] and Yuan Chen*[a]**

[a]School of Chemical and Biomedical Engineering, Nanyang Technological University, 62 Nanyang Drive, Singapore 637459

*Tel:+65-63168939; E-mail: chenyuan@ntu.edu.sg*

## 1. Experimental methods

### 1.1 Catalyst preparation

Three $Co/SiO_2$ catalysts with 1 wt.% Co were prepared by the impregnation method using three Co precursors, including cobalt (II) acetylacetonate ($Co(acac)_2$, Sigma-Aldrich, 97%), Co (II) chloride ($CoCl_2$, Alfa Aesar, 97%), and Co (II) nitrate hexahydrate ($Co(NO_3)_2 \cdot 6H_2O$, Sigma-Aldrich, 99.999%). $Co(acac)_2$ was dissolved in dichloromethane (Sigma-Aldrich, anhydrous, ≥99.8%), while $Co(NO_3)_2 \cdot 6H_2O$ and $CoCl_2$ was dissolved in deionized water. The Co precursor solutions were then added to fumed silicon dioxide powders (Cab-O-Sil, M-5, Sigma-Aldrich) with surface area of 254 $m^2/g$. The mixtures were aged at room temperature for 1 h, and subsequently dried in an oven at 100 °C for 2h. The dried catalyst was further calcined under airflow of 20 sccm per gram of catalyst from room temperature to 400 °C at 1 °C/min, and then kept at 400°C for 1 h. These three catalysts were denoted as $CoACAC/SiO_2$, $CoN/SiO_2$, and $CoCl/SiO_2$. In order to dope S into $Co/SiO_2$ catalysts, the above calcined catalysts were impregnated by dilute sulphuric acid ($H_2SO_4$, 0.04 mol/L) at the 8 mL solution/g catalyst ratio for 1 h. Afterwards, the mixtures were dried and calcined again using the same procedure described above. The resulting S doped catalysts were denoted as $CoACAC/SiO_2/S$, $CoN/SiO_2/S$, and $CoCl/SiO_2/S$, respectively.

### 1.2 SWCNT growth

SWCNTs were synthesized in a CVD reactor under the same condition for all catalysts. A catalyst was first reduced under pure $H_2$ (1 bar, 50 sccm) from room temperature to 540 $^{o}$C at 20 °C/min, and then further heated to 780 $^{o}$C under an Ar flow (1 bar, 50 sccm). At 780 $^{o}$C, pressured CO (6 bar, 200 sccm) replaced Ar and growth lasted for 1 h. The carbonyls in CO were removed by a Nanochem Purifilter from Matheson Gas Products.

### 1.3 SWCNT characterization

As-synthesized SWCNTs with catalysts were first dissolved in NaOH aqueous solution (1.5 mol/L) to remove $SiO_2$, and then filtered on a nylon membrane with 0.2 $\mu$m pores. Carbon deposits on filter membranes were further dispersed in 2 wt. % sodium dodecyl benzene sulphonate (SDBS, Aldrich) $D_2O$ solution by sonication using a cup-horn ultrasonicator (SONICS, VCX-130) at 20 W for 1 h. SWCNT suspension obtained after centrifugation at 50,000 g for 1 h was characterised by photoluminescence (PL) and UV–vis–near-infrared (UV–vis–NIR) absorption spectroscopies. PL was conducted on a spectrofluorometer (Jobin-Yvon, Nanolog-3) with the excitation scanned from 450 to 950 nm and the emission collected from 900 to 1600 nm. The UV–vis–NIR absorption spectra were collected from 500 to 1600 nm on a spectrophotometer (Varian Cary 5000). As-synthesized SWCNTs with catalysts and SWCNTs filtered on nylon membranes after $SiO_2$ removal were both characterized by Raman spectroscopy. No significant differences were found on the two types of samples. Raman spectra were collected on a Ramanscope (Renishaw) in the backscattering configuration over several random spots on each sample under 514 and 785 nm laser excitations. The integration time of 10 s. Laser energy of 2.5–5 mW was used to prevent sample damages.

### 1.4 Catalyst characterization

The physicochemical properties of catalysts were evaluated by elemental analysis, $H_2$–temperature programmed reduction ($H_2$–TPR), and UV–vis diffuse reflectance spectroscopy. First, the weight fraction of S in the doped catalysts was determined by an elemental analyzer (Elementarvario, CHN). Around 5 mg of catalyst sample was used for each test. Each type of catalyst was tested three times to obtain the average value. Before each test, all samples were dried at 100 $^{o}$C overnight. Next, the reducibility of Co species on undoped and S doped $Co/SiO_2$ catalysts was characterised by TPR. CoO (Sigma-Aldrich, 99.99%), $Co_3O_4$ (Sigma-Aldrich, 99.8%), $CoSiO_3$ (MP Biomedicals, ICN215905), $CoCl_2$ (Alfa Aesar, 97%), and $CoSO_4 \cdot 7H_2O$ (Sigma-Aldrich, 99%) were used as references for TPR analysis. Our TPR experimental setup was equipped with a thermal conductivity detector (TCD) of a gas chromatography (Techcomp 7900). An acetone–liquid $N_2$ trap was installed between a quartz cell and the TCD to condense

water or $H_2S$ produced during catalyst reduction. In each test, 200 mg of catalysts or reference samples with equivalent Co loadings were loaded into a quartz cell. 5% $H_2$ in Ar was introduced to the quartz cell at 30 sccm, and pure Ar gas was used as a reference for the TCD. After the TCD baseline was stable, the temperature of the quartz cell was increased to 950 $^oC$ at 5 $^oC$/min, and then held at 950 $^oC$ for 30 min. Last, UV–vis diffuse reflectance spectra of catalysts and Co reference samples were recorded on the spectrophotometer (Varian Cary 5000). The samples were first dried at 100 $^oC$ for 3 h, and then UV-vis spectra were recorded in the range of 200–800 nm with $BaSO_4$ as a reference.

## 2. Abundance of (*n,m*) species identified in PL

**Table S1.** Tabulated values of PL intensities and relative abundances of (*n,m*) species in SWCNTs produced on the CoACAC/$SiO_2$/S catalyst.

| (*n,m*) index | Diameter $d_t$ (nm) | Chiral angle $\theta$ (°) | $E_{11}$ (nm) | $E_{22}$ (nm) | PL intensity (counts) | Relative abundance,(%) |
|---|---|---|---|---|---|---|
| (*6,5*) | 0.76 | 27.00 | 983 | 570 | 537.5 | 7.7 |
| (*7,3*) | 0.71 | 17.00 | 990 | 510 | 264.9 | 3.8 |
| (*7,5*) | 0.83 | 24.50 | 1023 | 642 | 155.0 | 2.2 |
| (*7,6*) | 0.90 | 27.46 | 1122 | 646 | 169.5 | 2.4 |
| (*8,4*) | 0.84 | 19.11 | 1111 | 578 | 241.0 | 3.4 |
| (*8,6*) | 0.97 | 25.28 | 1165 | 714 | 113.5 | 1.6 |
| (*8,7*) | 1.03 | 27.80 | 1264 | 726 | 403.8 | 5.8 |
| (*9,7*) | 1.10 | 25.87 | 1321 | 790 | 995.2 | 14.2 |
| (*9,8*) | 1.17 | 28.05 | 1414 | 822 | 2836.2 | 40.5 |
| (*10,6*) | 1.11 | 21.79 | 1380 | 754 | 535.4 | 7.7 |
| (*10,8*) | 1.24 | 26.30 | 1467 | 870 | 277.0 | 4.0 |
| (*10,9*) | 1.31 | 28.30 | 1562 | 886 | 469.5 | 6.7 |

**Table S2.** Tabulated values of PL intensities and relative abundances of (*n,m*) species in SWCNTs produced on the CoCl/$SiO_2$/S catalyst.

| (*n,m*) index | Diameter $d_t$ (nm) | Chiral angle $\theta$ (°) | $E_{11}$ (nm) | $E_{22}$ (nm) | PL intensity (counts) | Relative abundance,(%) |
|---|---|---|---|---|---|---|
| (*6,5*) | 0.76 | 27.00 | 982 | 570 | 182.4 | 12.4 |
| (*7,3*) | 0.71 | 17.00 | 986 | 502 | 131.6 | 8.9 |
| (*7,5*) | 0.83 | 24.50 | 1023 | 642 | 96.1 | 6.5 |

| | | | | | | |
|---|---|---|---|---|---|---|
| (*7,6*) | 0.90 | 27.46 | 1113 | 642 | 72.3 | 4.9 |
| (*8,4*) | 0.84 | 19.11 | 1109 | 578 | 75.4 | 5.1 |
| (*8,6*) | 0.97 | 25.28 | 1162 | 714 | 49.0 | 3.3 |
| (*8,7*) | 1.03 | 27.80 | 1265 | 722 | 59.5 | 4.0 |
| (*9,7*) | 1.10 | 25.87 | 1319 | 790 | 106.6 | 7.2 |
| (*9,8*) | 1.17 | 28.05 | 1412 | 818 | 478.2 | 32.7 |
| (*10,6*) | 1.11 | 21.79 | 1376 | 758 | 63.2 | 4.3 |
| (*10,8*) | 1.24 | 26.30 | 1469 | 866 | 36.4 | 2.5 |
| (*10,9*) | 1.31 | 28.30 | 1558 | 890 | 119.9 | 8.2 |

**Table S3.** Tabulated values of PL intensities and relative abundances of (*n,m*) species in SWCNTs produced on the $CoN/SiO_2/S$ catalyst.

| (*n,m*) index | Diameter $d_t$ (nm) | Chiral angle $\theta$ (°) | $E_{11}$ (nm) | $E_{22}$ (nm) | PL intensity (counts) | Relative abundance,(%) |
|---|---|---|---|---|---|---|
| (*6,5*) | 0.76 | 27.00 | 979 | 566 | 228.4 | 8.8 |
| (*7,3*) | 0.71 | 17.00 | 986 | 506 | 135.4 | 5.2 |
| (*7,5*) | 0.83 | 24.50 | 1024 | 642 | 121.8 | 4.7 |
| (*7,6*) | 0.90 | 27.46 | 1113 | 642 | 101.6 | 3.9 |
| (*8,4*) | 0.84 | 19.11 | 1110 | 578 | 120.8 | 4.7 |
| (*8,6*) | 0.97 | 25.28 | 1165 | 714 | 63.9 | 2.5 |
| (*8,7*) | 1.03 | 27.80 | 1263 | 726 | 120.6 | 4.7 |
| (*9,7*) | 1.10 | 25.87 | 1319 | 790 | 259.1 | 10.0 |
| (*9,8*) | 1.17 | 28.05 | 1413 | 818 | 1020.8 | 39.5 |
| (*10,6*) | 1.11 | 21.79 | 1377 | 750 | 143.7 | 5.6 |
| (*10,8*) | 1.24 | 26.30 | 1469 | 866 | 81.5 | 3.1 |
| (*10,9*) | 1.31 | 28.30 | 1558 | 886 | 189.4 | 7.3 |

## 3. Raman spectra of SWCNTs

Fig. S1 shows Raman spectra of carbon deposits grown from undoped and S doped $Co/SiO_2$ catalysts under 514 and 785 nm laser excitations. The radial breathing mode (RBM) peaks (below 400 $cm^{-1}$), D band and G band features can be used to evaluate the diameter and quality of resulting SWCNTs.[1] The intense RBM peaks and weak D band peaks from carbon deposits grown on $CoCl/SiO_2$ and $CoACAC/SiO_2$ suggest that high quality SWCNTs are produced. In contrast, the low intensity RBM peaks and intense D band peaks from carbon deposits grown on $CoN/SiO_2$ suggest that this catalyst is not active for SWCNT growth. The RBM peaks can be correlated with the (*n,m*) structures of

SWCNTs according to the Kataura plot computed by the tight-binding model.[2] We calculated the diameter of SWCNTs using the equation $\omega_{RBM}$=223.5 $cm^{-1}/d_t$+12.5 $cm^{-1}$, where $\omega_{RBM}$ and $d_t$ are the RBM frequency and the diameter of SWCNTs.[3] The RBM peaks in Fig. S1a and 1c at 238 and 267 $cm^{-1}$ can be assigned to (*8,6*) and (*7,6*) according to the empirical Kataura plot,[3] suggesting that the undoped catalysts mainly produce SWCNTs with diameters less than 1 nm. In comparison, all S doped $Co/SiO_2$ catalysts produce SWCNTs with high quality, as indicated by their intense RBM peaks and weak D band peaks (see Fig. S1b and S1d). The major RBM peaks centered around 202 and 213 $cm^{-1}$ can be ascribed to the (*9,8*) and (*9,7*) with diameters around 1.1–1.17 nm.

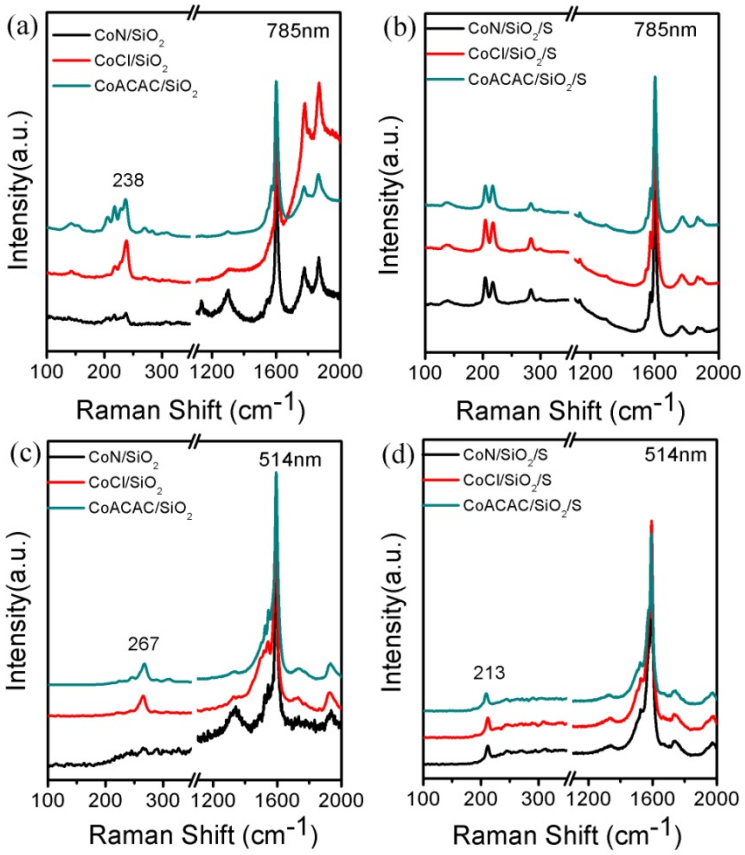


**Fig. S1** Raman spectra of SWCNTs grown on undoped $Co/SiO_2$ catalysts (a and c) and S doped $Co/SiO_2$ (b and d) under 785 and 514 nm laser excitations, respectively. The regions on the left correspond to RBM peaks, while the regions on the right correspond to D and G bands.

## 4. UV-vis spectra of $Co/SiO_2$ catalysts

UV–vis diffuse reflectance spectroscopy was used to study the surface chemistry of undoped and S doped $Co/SiO_2$ catalysts. Fig. S2 shows that the spectrum of $CoN/SiO_2$ is similar to that of $Co_3O_4$, having two broad peaks at around 400 and 720 nm, respectively. These two peaks can be assigned to the $\nu_1\ ^4A_{1g}\rightarrow{}^1T_{1g}$ and $\nu_2\ ^1A_{1g}\rightarrow{}^1T_{2g}$ transitions of octahedral configured $Co^{3+}$ ions.[4] The spectrum of $CoCl/SiO_2$ shows two broad peaks around 550 and 720 nm, which suggests the presence of $CoO_X$ and $CoCl_2$. $CoACAC/SiO_2$ has two peaks around 570 and 650 nm, suggesting the formation of surface Co silicates.[5] In contrast, the three S doped $Co/SiO_2$ catalysts all have a broad peak around 535 nm similar to that of $CoSO_4$, suggesting the existence of Co species bonded to $SO_4^{2-}$. We also found that all of them have a similar light pink color.

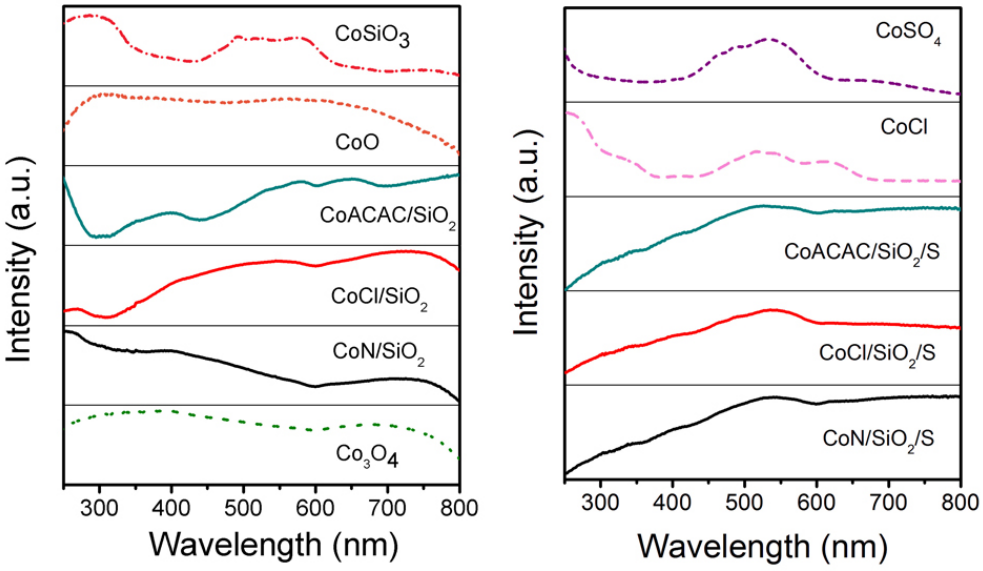


**Fig. S2** UV–vis diffuse reflectance spectra: (a) Co/SiO2 catalysts and references ($Co_3O_4$, CoO and CoSiO3), (b) S doped Co/SiO2 catalysts as well as the reference CoCl and $CoSO_4$.

## 5. Transmission Electron Microscopy (TEM) images

One milligram of as-synthesized SWCNTs together with the catalyst ($CoACAC/SiO_2/S$) was sonicated with 5 mL of anhydrous ethanol for 1 h, and a drop of the suspension was applied to a copper grid with holey carbon film. The grid was inserted into a Philips Tecnai 12 electron microscope, and TEM images were taken at an operation voltage of 120 kV. TEM images in Fig. S3 shows that SWCNTs grown from Co nanoparticles on $SiO_2$ form nanotube bundles. The diameter of individual tubes is about 1.2 nm, which agrees with spectroscopic results. Because active Co nanoparticles would

be embedded under or near $SiO_2$ surface, we are still unable to quantify their size and composition in TEM analysis.

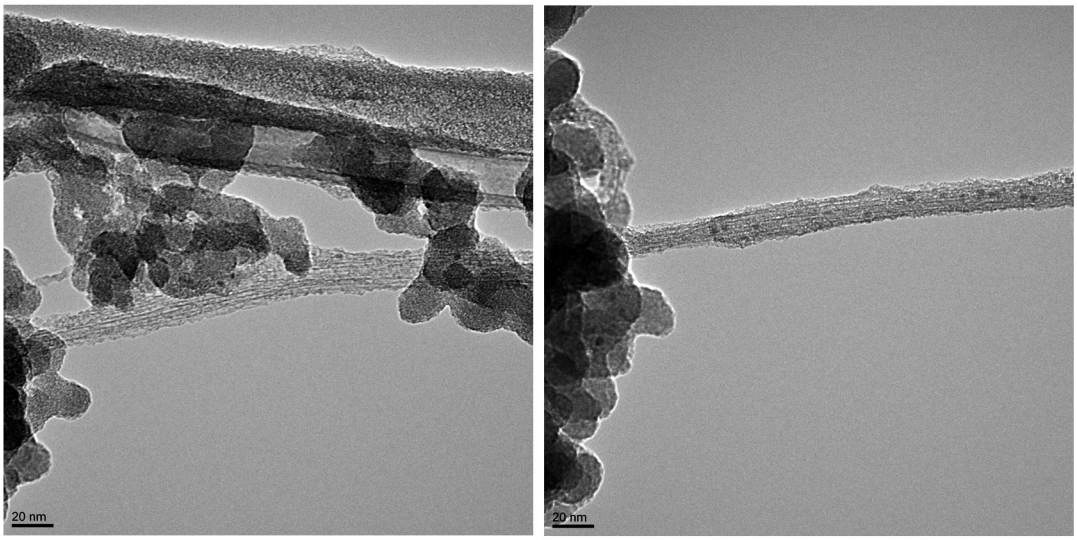


**Fig. S3** TEM images of SWCNTs and catalyst particles.

## 6. $(NH_4)_2SO_4$ doped $Co/SiO_2$ catalyst

### 6.1 Doping method

The $CoN/SiO_2$ catalyst was impregnated by ammonium sulfate ($(NH_4)_2SO_4$, 0.2 mol/L) at the 8 mL solution/g catalyst ratio for 1 h, and subsequently dried in an oven at 100 °C for 2 h. The dried catalyst was further calcined under air flow of 20 sccm per gram of catalyst from room temperature to 400 °C at 1 °C/min, and then kept at 400 °C for 1 h. The resulting S doped catalyst was denoted as $CoN/SiO_2/AS$.

### 6.2 PL and abundance of (n,m) species

The PL map in Fig. S4 shows that $(NH_4)_2SO_4$ doped $CoN/SiO_2$ catalyst produces dominantly (*6,5*) tubes (35.4 %) while (*9,8*) tubes are present in smaller amount (11.3 %). This can be attributed to the doping of S. Overall, $CoN/SiO_2/AS$ is less selective to (9,8) SWCNTs as compared to $CoN/SiO_2/S$.

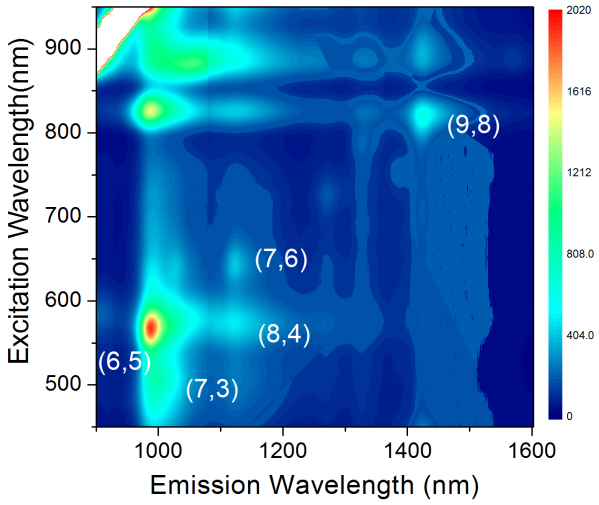


**Fig. S4** PL map of SDBS-dispersed SWCNTs grown on the CoN/$SiO_2$/AS catalyst.

**Table S4.** Tabulated values of PL intensities and relative abundances of (*n,m*) species in SWCNTs produced on the CoN/$SiO_2$/AS catalyst.

| (*n,m*) index | Diameter $d_t$ (nm) | Chiral angle $\theta$ (°) | $E_{11}$ (nm) | $E_{22}$ (nm) | PL intensity (counts) | Relative abundance,(%) |
|---|---|---|---|---|---|---|
| (*6,5*) | 0.76 | 27.00 | 991 | 566 | 1928.3 | 35.40% |
| (*7,3*) | 0.71 | 17.00 | 989 | 502 | 734.1 | 13.50% |
| (*7,5*) | 0.83 | 24.50 | 1025 | 638 | 408.4 | 7.50% |
| (*7,6*) | 0.90 | 27.46 | 1127 | 642 | 409.7 | 7.50% |
| (*8,4*) | 0.84 | 19.11 | 1120 | 574 | 486.4 | 8.90% |
| (*8,6*) | 0.97 | 25.28 | 1163 | 718 | 138.3 | 2.50% |
| (*8,7*) | 1.03 | 27.80 | 1269 | 726 | 173.7 | 3.20% |
| (*9,7*) | 1.10 | 25.87 | 1330 | 790 | 216.7 | 4.00% |
| (*9,8*) | 1.17 | 28.05 | 1428 | 822 | 613.6 | 11.30% |
| (*10,6*) | 1.11 | 21.79 | 1377 | 754 | 123.1 | 2.30% |
| (*10,8*) | 1.24 | 26.30 | 1470 | 866 | 105.7 | 1.90% |
| (*10,9*) | 1.31 | 28.30 | 1557 | 890 | 107.2 | 2.00% |

### 6.3 Absorption spectra

The strong absorption peaks at 1415 and 810 nm in Fig. S5 correspond to the $E^S_{11}$ and $E^S_{22}$ transition of (*9,8*). The peak around 983 nm from the $E^S_{11}$ transition of (6,5) is much more intense compared to that of SWCNTs grown from CoN/$SiO_2$/S, indicating more (6,5) tubes are grown on CoN/$SiO_2$/AS. As the absorption coefficient of (9,8) is higher than that of (6,5), the absorption peaks from (9,8) look larger than that of (6,5). A few

absorption peaks below 700 nm can be assigned to either the $E^{M}_{11}$ transition of metallic (*9,6*) and (*10,10*) or the $E^{S}_{22}$ transition of semiconducting (*6,5*).

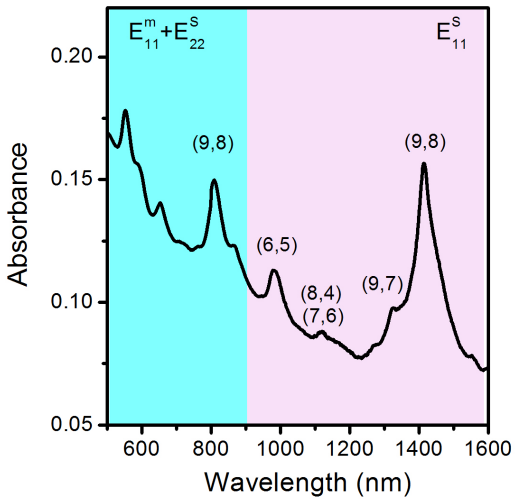


**Fig. S5** UV–vis-NIR absorption spectra of SDBS-dispersed SWCNTs grown on $CoN/SiO_2/AS$.

### 6.4 $H_2$–TPR

The TPR profile of $CoN/SiO_2/AS$ has an intense peak around 519 °C, which is similar to that of $CoN/SiO_2/S$ shown in Fig. 2c. However, the large peak around 800 $^{o}$C of $CoN/SiO_2/S$ shown in Fig. 2c is very weak in Fig. S6. The $CoN/SiO_2/AS$ has a broad peak from 425–800 $^{o}$C, suggesting the existence of several Co species, including unreacted $CoO_x$, Co hydrosilicate, and surface Co silicate.[6]

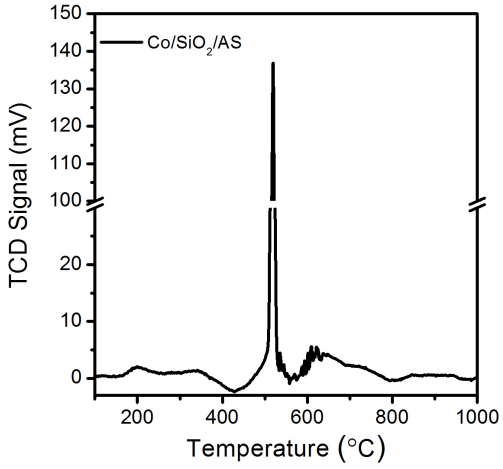


**Fig. S6** $H_2$–TPR profile of the $CoN/SiO_2/AS$ catalyst.

### 6.5 UV–vis diffuse reflectance spectroscopy

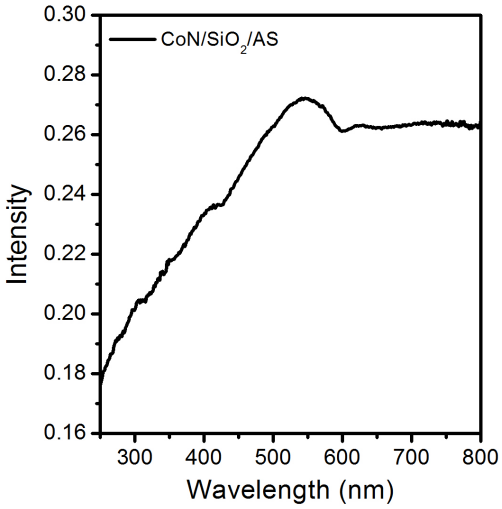


**Fig. S7** UV–vis diffuse reflectance spectrum of $CoN/SiO_2/AS$.

Fig. S7 shows that the UV–vis spectrum of $CoN/SiO_2/AS$ catalyst has a broad peak around 535 nm similar to that of $CoN/SiO_2/S$, suggesting the existence of Co species bonded to $SO_4^{2-}$.

## 7. References

1. M. S. Dresselhaus, G. Dresselhaus and A. Jorio, *J. Phys. Chem. C*, 2007, **111**, 17887–17893.
2. H. Kataura, Y. Kumazawa, Y. Maniwa, I. Umezu, S. Suzuki, Y. Ohtsuka and Y. Achiba, *Synth. Met.*, 1999, **103**, 2555-2558.
3. R. B. Weisman and S. M. Bachilo, *Nano Lett.*, 2003, **3**, 1235-1238.
4. Y. Brik, M. Kacimi, M. Ziyad and F. Bozon-Verduraz, *J. Catal.*, 2001, **202**, 118-128.
5. A. Khodakov, J. Girardon, A. Griboval-Constant, A. Lermontov and P. Chernavskii, *Stud. Surf. Sci. Catal.*, 2004, **147**, 295-300.
6. E. v. Steen, G. S. Sewell, R. A. Makhothe, C. Micklethwaite, H. Manstein, M. de Lange and C. T. O'Connor, *J. Catal.*, 1996, **162**, 220-229.